Neuron, Vol. 35, 345–353, July 18, 2002, Copyright ©2002 by Cell Press

Subunit-Specific NMDA Receptor Trafficking to Synapses

Andres Barria and Roberto Malinow[1]
Cold Spring Harbor Laboratory
1 Bungtown Road
Cold Spring Harbor, New York 11724

Summary

To elucidate mechanisms controlling the number and subunit composition of synaptic NMDA-Rs in hippocampal slice neurons, the NR1, NR2A, and NR2B subunits were optically and electrophysiologically tagged. The NR2 subunit directs delivery of receptors to synapses with different rules controlling NR2A and NR2B. Synaptic incorporation of NR2B-containing receptors is not limited by synaptic transmission nor enhanced by increased subunit expression. NR2A-containing receptors whose expression normally increases with age replace synaptic NR2B-containing receptors. Replacement is enhanced by increased NR2A expression and requires synaptic activity. Surprisingly, spontaneously released transmitter acting on synaptic NMDA-Rs is sufficient for replacement and reduces NMDA-R responses. Thus, as with AMPA-Rs, synaptic trafficking of NMDA-Rs is tightly regulated and has subunit-specific rules with functionally important consequences.

Introduction

Synaptic NMDA-type glutamate receptors (NMDA-Rs) play critical roles during brain development, plasticity, and pathology (Constantine-Paton and Cline, 1998; Dingledine et al., 1999; Zoghbi et al., 2000). A number of studies indicate that different levels of synaptic NMDA-R activation with corresponding degrees of calcium influx can lead to multiple effects. Low levels of NMDA-R activation produce synaptic depression, while higher levels of activation produce synaptic potentiation (Cummings et al., 1996; Zucker, 1999). Even higher levels of activation can lead to cell death (Choi, 1995). Thus, the number and properties of NMDA-Rs at a synapse must be under careful control in order to allow the appropriate amount of calcium entry. The nature of this regulation and, specifically, the roles played by NMDA-R expression levels and synaptic activity in controlling the number and properties of synaptic NMDA-Rs is poorly understood.

In the hippocampus, NMDA-Rs are heteromultimeric complexes composed of the NR1 subunit and one or more of the two NR2 subunits, NR2A and NR2B (Sheng et al., 1994). Both NR1 and NR2 subunits are required to form a functional ionotropic receptor (Dingledine et al., 1999; Meguro et al., 1992; Monyer et al., 1992). The NR2B subunit is expressed prenatally and is required for normal neuronal pattern formation and viability of the animal (Kutsuwada et al., 1996), while the NR2A subunit progressively increases its expression (Monyer et al., 1994; Sheng et al., 1994) and synaptic incorporation (Stocca and Vicini, 1998; Tovar and Westbrook, 1999) with age. The different NR2 subunits confer different kinetic properties to the NMDA-R (Monyer et al., 1994), and it has been hypothesized that the change from NR2B to NR2A may be responsible for the decreased plasticity observed in older animals (Carmignoto and Vicini, 1992; Crair and Malenka, 1995). The mechanisms controlling the switch in the composition of synaptic NMDA-Rs from NR2B- to NR2A-containing receptors are not well understood.

The cytoplasmic carboxyl termini of synaptic receptors have been shown to play critical roles in directing the trafficking to and stabilization at synaptic sites (Calver et al., 2001; Mori et al., 1998; Osten et al., 2000; Pagano et al., 2001; Passafaro et al., 2001; Shi et al., 2001; Sprengel et al., 1998; Steigerwald et al., 2000). NR2A and NR2B both contain very long cytoplasmic termini (627 and 644 amino acids, respectively), including a PDZ binding motif at the very terminus, thereby enabling a potential for many protein-protein interactions. The NR1 cytoplasmic tail is more modest in length (105 amino acids or smaller), and the splice variant predominantly expressed in hippocampus (NR1-1a) has no PDZ binding motif (Laurie and Seeburg, 1994; Nakanishi et al., 1992). Given the proposed role of PDZ-domain proteins in targeting signaling molecules (Garner et al., 2000; Sheng and Pak, 2000) and the length of their cytoplasmic termini, the NR2 subunits are good candidates to participate in controlling the number and composition of NMDA-Rs at synapses.

Results

Imaging of GFP-Tagged NMDA-Rs

To examine receptor trafficking in neurons, NMDA-R subunits were tagged with GFP at their amino terminus and expressed in organotypic hippocampal slices (see Experimental Procedures). NR1-GFP (splice variant NR1-1a) was distributed throughout dendrites but was restricted from dendritic spines, the sites of excitatory contacts (Figure 1A). Coexpression of T1-Red and NR1-GFP revealed the presence of dendritic spines and confirmed the retention of this subunit in the dendritic shaft (Figure 1A). The subcellular distribution of NR1-GFP is consistent with the existence of an intracellular pool that is not assembled with NR2 subunits (Huh and Wenthold, 1999) and recent reports indicating retention of this NR1 splice form in endoplasmic reticulum (ER) (Scott et al., 2001; Standley et al., 2000; Xia et al., 2001). To determine if NR2 can drive NR1 into spines, we coexpressed NR1-GFP along with untagged NR2. Indeed, now NR1-GFP showed clear delivery to spines (Figures 1B and 1C), indicating that NR2 can drive NR1 to spines. The delivery of receptor into spines was quantified by measuring the fluorescence intensity at a spine and underlying dendritic shaft and computing the ratio (spine/dendrite, see Experimental Procedures). As shown in Figure 1D, NR1-GFP expressed alone is not detected at spines but coexpression of NR1-GFP with either NR2 subunit allows

[1]Correspondence: malinow@cshl.org

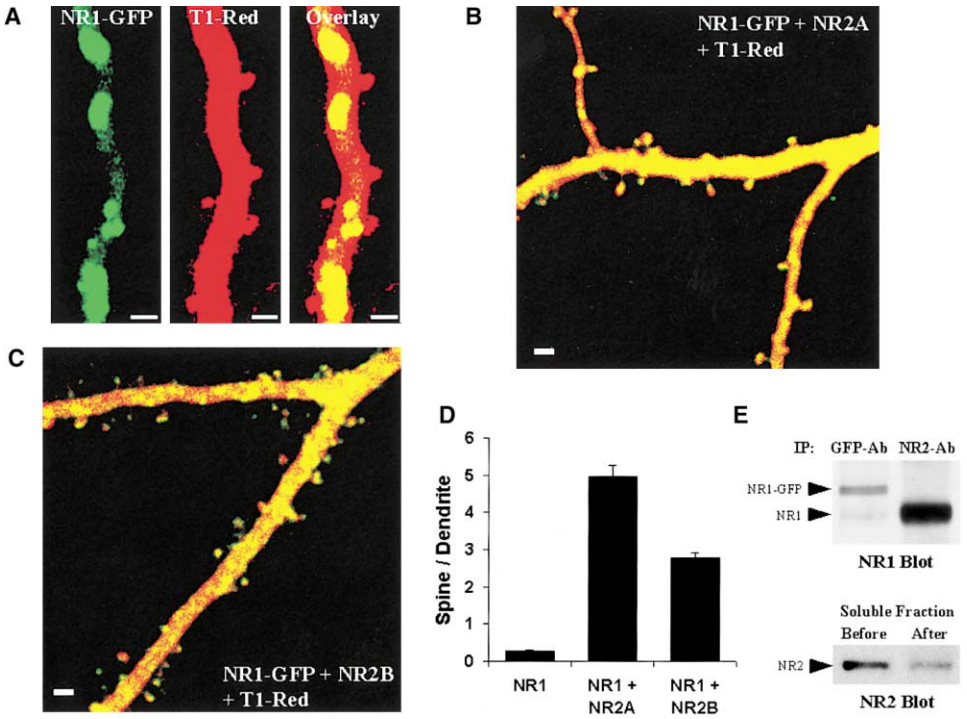

Figure 1. NR2 Subunits Can Deliver NR1-GFP Subunits into Spines

Two-photon scanning laser images of hippocampal slice CA1 neurons expressing GFP-tagged NMDA-R subunits.

(A) NR1-GFP does not reach dendritic spines. Apical dendritic region of a neuron cotransfected with (left) NR1-GFP and (middle) T1-Red to show cellular morphology. Right, overlap of green and red channels. Note clusters of NR1-GFP in the dendritic shaft with no delivery to spines.

(B) Overlap image of apical dendritic region of neuron cotransfected with NR1-GFP, NR2A, and T1-Red; note delivery of heteromers into dendritic spines.

(C) Overlap image of apical dendritic region of a neuron cotransfected with NR1-GFP, NR2B, and T1-Red; heteromers are delivered into dendritic spines.

(D) Quantification of GFP-tagged receptor present in dendritic spines. Ratio of spine/dendrite (see Experimental Procedures) for cells cotransfected with NR1-GFP and T1-Red (two cells, 159 spines); NR1-GFP, NR2A, and T1-Red (four cells, 164 spines); and NR1-GFP, NR2B, and T1-Red (two cells, 146 spines).

(E) NR1-GFP does not heteromerize with endogenous NR2 subunits. Slices expressing NR1-GFP were homogenized and immunoprecipitated with antibodies against GFP (left lane) or NR2-A/B (right lane) and probed with antibody against NR1 (top). Antibody against NR2-A/B immunoprecipitates >70% of NR2 (bottom) and coimmunoprecipitates endogenous NR1, but not NR1-GFP (top).

Bar = 2 μM.

delivery of the heterocomplex into spines. These results indicate that the NR2 subunit contains information that can relieve the apparent ER retention allowing delivery of NMDA-R complexes to dendritic spines.

Functional Insertion of Recombinant NMDA-R into Synapses

To monitor functional insertion of recombinant receptors into synaptic sites, we introduced an electrophysiological tag in NR1-GFP. Asparagine 598 was mutated to arginine, eliminating the Mg^{2+} blockade and Ca^{2+} permeability (Burnashev et al., 1992; Mori et al., 1992; Single et al., 2000). Thus, heteromers containing $NR1_{N598R}$-GFP exhibit a linear current-voltage relation when expressed in HEK-293 cells (Figure 2A). $NR1_{N598R}$-GFP and NR2A or NR2B were coexpressed in hippocampal slice neurons to study the trafficking of NMDA-R complexes into synapses. Excitatory postsynaptic currents (EPSCs) recorded from transfected neurons displayed a slow component at a holding potential of −60 mV. This late component was mediated by activation of recombinant NMDA-R as it was not present in nontransfected cells, was not affected by the AMPA-R blocker NBQX, and was abolished by the NMDA-R antagonist APV (Figure 2B). These results indicate that we can measure functional delivery of a recombinant NMDA-R to synapses. Notably, expression of $NR1_{N598R}$-GFP alone produced no such late component (Figures 2C and 2D), supporting our observation that NR1-GFP alone does not go into spines. The electrophysiological and imaging results with NR1-GFP suggest that recombinant NR1-GFP does not heteromerize with endogenous NR2 subunits. This is also confirmed by coimmunoprecipitation experiments. Endogenous NR1, but not NR1-GFP, was coimmunoprecipitated with NR2 antibody from slices expressing NR1-GFP (Figure 1E, top) when over 70% of NR2 subunit is immunoprecipitated (Figure 1E, bottom).

To begin to examine the structural motifs of receptors that may play a part in their delivery to synapses, we removed the PDZ binding regions of NR2 subunits, comprised of the last six amino acids of the cytoplasmic carboxyl-tail (Kornau et al., 1995; Sheng and Sala, 2001), to generate $NR2A_{\Delta PDZ}$ and $NR2B_{\Delta PDZ}$. Neurons express-

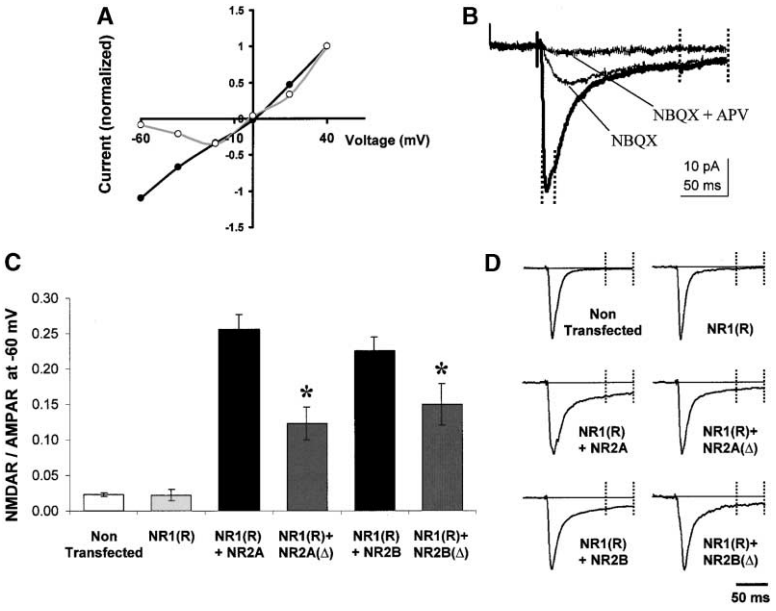

Figure 2. Electrophysiological Tag of NMDA-R Allows Monitoring of Functional Insertion of Recombinant Receptor into Synapses

(A) Point mutation on NR1 subunit eliminates Mg^{2+} blockade on NMDA-Rs (Burnashev et al., 1992; Mori et al., 1992; Single et al., 2000). I/V relationship of NMDA-activated currents in HEK-293 cells transfected with NR2A-GFP subunit and $NR1_{wt}$-GFP (open circles) or $NR1_{N598R}$-GFP (closed circles) in physiological solution with 4 mM Mg^{2+}. Currents were normalized by values obtained at +40 mV. A similar I/V curve was obtained with NR2B-GFP-containing receptors (data not shown).

(B) Delivery of recombinant NMDA-Rs to synapses is detected as a late component in the EPSC at a holding potential of −60 mV. Average responses from cell transfected with $NR1_{N598R}$-GFP/NR2A-GFP at a holding potential of −60 mV. The late component was not blocked by NBQX (2 μM) but is blocked by APV (100 μM). Dashed lines indicate windows used to measure AMPA and NMDA responses.

(C) Only heteromers of $NR1_{N598R}$-GFP and NR2-GFP subunits are detected at synapses. Graph plotting the amount of recombinant NMDA-R detected electrophysiologically at synapses after expression of different NMDA-R subunits, as indicated. Synaptic delivery is calculated as the ratio of NMDA to AMPA synaptic currents recorded at −60 mV. No apparent synaptic delivery of $NR1_{N598R}$-GFP alone (NR1[R]; n = 21, not significantly different from nontransfected cells n = 22, $p > 0.05$). Coexpression of $NR1_{N598R}$-GFP and NR2A-GFP or NR2B-GFP show clear delivery of the receptor to synapses (n = 43, $p < 0.01$; n = 26, $p < 0.01$, respectively). Deletion of PDZ binding domain reduces, but does not block, delivery of recombinant NMDA-R. The average ratio of late to early synaptic component was diminished in cells expressing receptors containing $NR2A_{\Delta PDZ}$ (NR2A[Δ]; n = 29, p = 0.002) and $NR2B_{\Delta PDZ}$ (NR2B[Δ]; n = 26, p = 0.03).

(D) Examples of peak-normalized average responses recorded at −60 mV.

ing $NR1_{N598R}$-GFP and $NR2A_{\Delta PDZ}$ or $NR2B_{\Delta PDZ}$ showed reduced delivery of recombinant receptors to synapses (Figure 2C). This suggests a role for the PDZ binding regions of the NR2 subunits in the incorporation or stabilization of the receptor at synapses. Since NR1-GFP does not heteromerize with endogenous NR2 subunits (see above), it is unlikely that wild-type NR2 subunits get incorporated in the heterocomplex containing recombinant $NR1_{N598R}$-GFP and $NR2A_{\Delta PDZ}$ or $NR2B_{\Delta PDZ}$. This suggests that domains other than the PDZ binding regions are sufficient to deliver NMDA-Rs to synapses, albeit with lower efficacy.

Role of Synaptic Activity in the Trafficking of NMDA-Rs

To study the effect of neural activity on NMDA-R trafficking, we incubated slices from the time of transfection to the time of recording in either tetrodotoxin (TTX) (1 μM, to block action potentials), high Mg^{2+} (10 mM, to depress synaptic function; Zhu et al., 2000), or NBQX (2 μM, to block AMPA receptors). None of these treatments prevented the synaptic insertion of recombinant receptors containing $NR1_{N598R}$-GFP, and either NR2A or NR2B to synapses (Figures 3A and 3B). Surprisingly, treatment of slices with 100 μM APV (an NMDA-R antagonist that competes at the glutamate binding site) or 100 μM 5,7-dichlorokynurenic acid (an antagonist at the glycine binding site of NMDA-Rs) did prevent the insertion of NR2A-containing receptors into synapses (Figure 3A). Neither APV nor 5,7-dichlorokynurenic acid blocked synaptic delivery of NR2B-containing receptors (Figure 3B). Treatment of slices with MCPG (to block metabotropic glutamate receptors) also had no effects on synaptic insertion of NR2B-containing receptors (Figure 3B). Together, these results indicate that insertion of NR2A-containing receptors into synapses requires activation of synaptic NMDA-Rs. However, spontaneously released glutamate, as it occurs in the presence of TTX, appears to be sufficient to effect synaptic insertion of NR2A-containing receptors. To test if spontaneous release of glutamate produces electrophysiologically detectable NMDA-R-mediated responses, we examined the effects of APV on spontaneously recorded responses. As shown in Figure 4, spontaneous synaptic responses recorded in the presence of TTX plus NBQX or high Mg^{2+} were not affected by APV (Figures 4B, 4D, and 4F). This suggests that little, if any, NMDA-R-mediated currents are produced in the presence of TTX, NBQX, or high Mg^{2+}. Thus, it is likely that only ligand binding to synaptic NMDA-Rs is sufficient to bring NR2A-containing receptors to synapses. This conclusion is supported by results with ketamine, an NMDA-R antagonist that blocks channel conductance, but not ligand binding (MacDonald et al., 1991). While ketamine blocked NMDA-R currents (200 μM: 93%, n = 6), slices maintained in the drug showed robust synaptic delivery of $NR1_{N598R}$-GFP and NR2A (Figure 3A). Such regulation resulting from ligand binding is consistent with recent results showing use-dependent internalization of NMDA-R in heterologous systems (Vissel et al., 2001). In contrast, synaptic insertion of functional NR2B-containing receptors seems not to require activation of glutamate receptors (Figure 3B).

We also examined the different effects of activity on trafficking of NR2A- and NR2B-containing receptors, using fluorescent tags. Slices expressing NR1 and NR2A

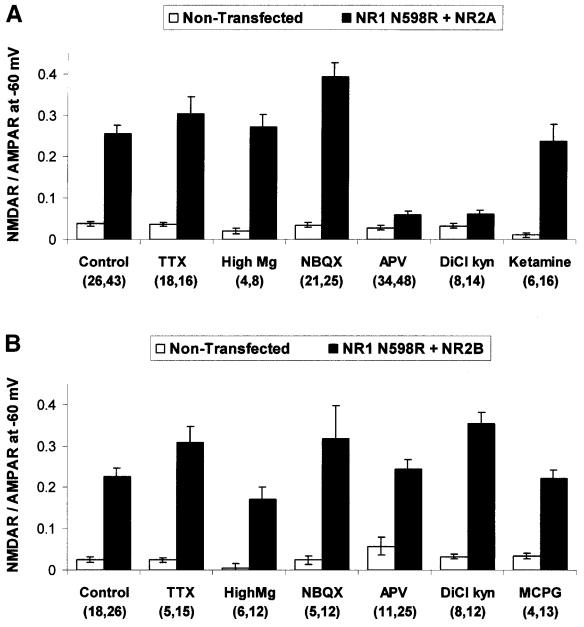

Figure 3. Ligand Binding, But Not Ion Flux, Is Required for Synaptic Delivery of NR2A-Containing Receptors

(A) Graph showing synaptic delivery of recombinant receptor, measured as the ratio of NMDA to AMPA synaptic current, recorded at –60 mV. Slices transfected with $NR1_{N598R}$-GFP/NR2A-GFP were maintained in normal culture medium (control) or culture medium plus TTX (1 μM), high Mg^{2+} (10 mM), NBQX (2 μM), APV (100 μM), 5,7 diclorokynurenic acid (100 μM), or ketamine (200 μM). Drugs were replenished every day. Recordings from nontransfected (open bars) and transfected (closed bars) cells were obtained in normal ACSF (number of cells for each group indicated in parentheses).

(B) Same as (A) plus MCPG (1 mM) for slices transfected with $NR1_{N598R}$-GFP/NR2B-GFP. Synaptic delivery of recombinant NR2A-containing receptors, but not NR2B-containing receptors, was blocked by APV or 5,7 diclorokynurenic acid.

subunits were maintained with APV during the period of expression. Transfected neurons showed increased concentration of receptor at spines compared with control slices (no treatment). This suggests that under these conditions, receptors accumulate at spines without being functionally inserted at the synapse (Figures 5A and 5B). Similar optical accumulation in spines has been observed with AMPA-Rs that cannot incorporate into synapses (e.g., homomeric GluR3; Shi et al., 2001) and homomeric GluR2 with PDZ-domain mutation (Piccini and Malinow, 2002). Our electrophysiology results above suggest that blockade of ligand binding onto synaptic NMDA-Rs, rather than blockade of current flux, is responsible for the aberrant trafficking. We tested this with MK-801, an NMDA-R channel blocker. Indeed, while APV induced spine accumulation of NR2A-containing receptors, MK-801 did not (Figures 5A–5C). This confirms that opening of synaptic NMDA-R channels is not necessary for normal trafficking of NR2A-containing receptors, supporting a model where only ligand binding is required. As expected, APV treatment did not have an effect on distribution of NR1wt-GFP coexpressed with NR2B (Figures 5D and 5E).

Incorporation of NR2A-Containing Receptors at Synapses

These results, together with the previously described developmental expression pattern of NR2B and NR2A (Chavis and Westbrook, 2001; Monyer et al., 1994; Sheng et al., 1994; Tovar and Westbrook, 1999; Vissel et al., 2001), suggest a model where synapses first acquire NR2B-containing receptors in an activity-independent manner. As NR2A increases in expression and if ligand binds to NR2B-containing receptors on synapses, these receptors are internalized and replaced by NR2A-containing receptors. To examine directly if an increase in NR2A expression can drive replacement of synaptic NR2B-containing receptors, we compared NMDA-R responses between nearby nontransfected neurons and neurons expressing (wild-type) NR1-GFP and NR2A. NMDA-R responses in transfected cells showed faster decay (Figure 6A), consistent with synaptic incorporation of NR2A-containing receptors, which have a faster decay-time than NR2B-containing receptors (Dingledine et al., 1999; Flint et al., 1997; Monyer et al., 1994). Interestingly, responses in cells transfected with NR1-GFP and NR2A became largely insensitive to the NR2B-blocking drug ifenprodil (Williams, 1993) (Figure 6A, hatched bars). This indicates effective replacement of endogenous NR2B-containing synaptic receptors with recombinant NR2A-containing receptors. As expected, if slices were maintained in APV during expression of recombinant NR2A and NR1-GFP, the change in decay time was not observed (Figure 6B), indicating no incorporation of recombinant receptor into synapses. This suggests that wild-type recombinant receptors behave as the pore mutant receptors and that the difference in single-channel conductance, increase in voltage-independent sodium influx, and loss of calcium permeability in pore mutant receptors (Burnashev et al., 1992; Mori et al., 1992; Single et al., 2000) does not affect their trafficking. Of note, neurons expressing NR1-GFP and NR2A showed significantly depressed NMDA-R synaptic responses compared to nearby nontransfected cells (Figures 6C and 6D). Again, this effect was blocked when slices were kept in APV during the expression period (data not shown). Thus, increased expression of NR2A leads to effective removal of synaptic NR2B, synaptic incorporation of NR2A, and significant reduction of synaptic NMDA-R currents. These modifications are promoted by increased NR2A expression but still require synaptic activity for them to be effected.

To test if increased expression of NR2B had effects similar to those of NR2A, we examined transmission onto cells expressing NR1-GFP and NR2B. These transfected neurons were no different from nearby nontransfected cells with respect to timecourse or amplitude of NMDA-R-mediated synaptic responses (Figures 7A–7C). Since these neurons do have synaptic NR2A-containing receptors, as indicated by an incomplete block of NMDA-R currents by ifenprodil (Figure 7D), this indicates that NR2B-containing receptors do not replace synaptic NR2A-containing receptors. Furthermore, since the amplitude of synaptic responses is not larger in transfected cells, increased expression of NR2B does not increase the number of synaptic NR2B-containing receptors,

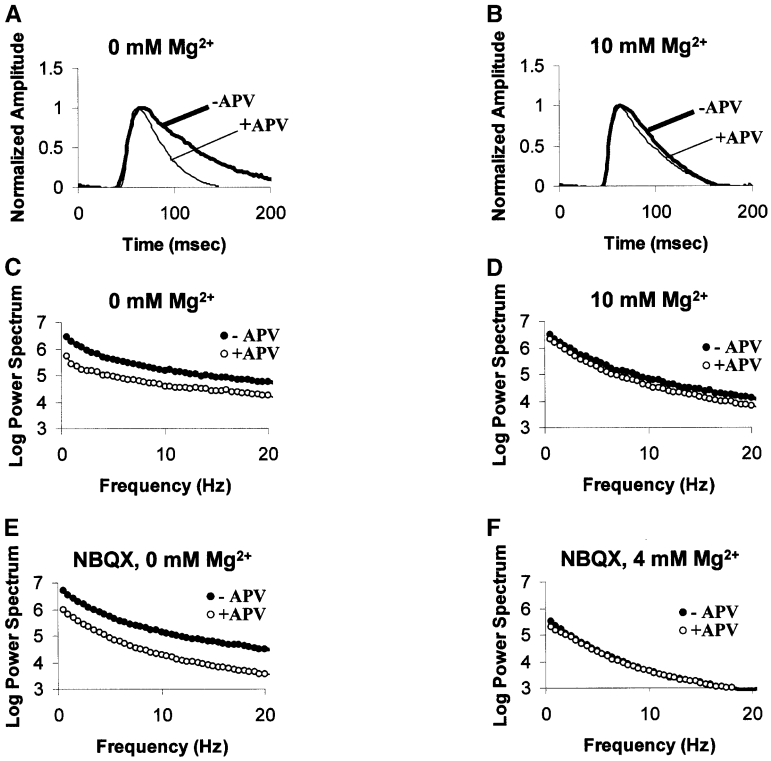

Figure 4. TTX, High Mg^{2+}, and NBQX Block Current through NMDA Receptors in Miniature Synaptic Events

(A and B) Averages of miniature EPSPs (>100 each) evoked in the presence of TTX (1 μM) with puffed 0.5 M sucrose recorded from nontransfected cells in ACSF without Mg^{2+} (A) (to demonstrate events with NMDA-R component) or 10 mM Mg^{2+} (B). Thin line is average of events after APV (100 μM) has been added to the bath.

(C and D) Power spectrum of spontaneous activity in ACSF with 10 mM Mg^{2+} (D) or without Mg^{2+} in the absence of APV (C) (closed circles) or after APV (open circles).

(E and F) Power spectra of spontaneous activity in normal ACSF (4 mM Mg^{2+}) plus NBQX (F) (2 μM) or ACSF without Mg^{2+} plus NBQX before APV (closed circles) or after APV has been added to the bath (E) (open circles). Note that APV produces no effects on responses measured in high Mg^{2+} or NBQX and normal Mg^{2+}, while APV shows clear effects on responses measured in low Mg^{2+}, indicating that high Mg^{2+} or NBQX effectively block spontaneously activated NMDA currents.

consistent with previous reports using transgenic animals (Philpot et al., 2001b).

Discussion

We have developed optical and electrophysiological tags to examine incorporation of NMDA-R to synapses in hippocampal slices. When expressed alone, NR1-1a, which contains no PDZ domain, is largely retained in the dendritic shaft away from synapses. We show that NR2 subunits contain information that relieves this retention, allowing the receptor to be inserted at synapses. The PDZ domain on NR2 is partly, but not completely, responsible for this relief and synaptic insertion. This is consistent with previous results implicating PDZ-domain proteins (in that case binding to NR1 splice variants different from the one in this study) in the relief of ER retention observed in heterologous systems (Scott et al., 2001; Standley et al., 2000; Xia et al., 2001) and the cytoplasmic tail of NR2 subunits in the synaptic localization of NMDA-Rs (Mori et al., 1998; Steigerwald et al., 2000).

Our studies indicate that increased expression of NMDA-R subunits does not increase the number of receptors at synapses, but can affect the composition of receptors at synapses and decrease the synaptic NMDA-R response. Insertion of NMDA-R into synaptic sites follows different rules, depending on receptor subunit composition. Synaptic insertion of NR2B-containing receptors does not increase with increased levels of expression nor does it require glutamatergic synaptic activity. It is possible that apposition of the presynaptic terminal or release of other substances (Dalva et al., 2000) can control synaptic insertion of NR2B-containing receptors. Synthesized NR2B-containing receptors replace synaptic NR2B-containing receptors, but not synaptic NR2A-containing receptors. In contrast, synaptic insertion of NR2A-containing receptors requires synaptic activity, is promoted by increased levels of NR2A expression, and replace synaptic NR2B-containing receptors. Our data support a model (Figure 8) in which newly formed synapses initially acquire NR2B-containing receptors in a manner not requiring glutamatergic transmission. As NR2A expression increases, either through a developmental program or increased neural activity (Quinlan et al., 1999), NR2B-containing receptors can be replaced by NR2A-containing receptors. This replacement is use-dependent, consistent with in vivo (Carmignoto and Vicini, 1992; Quinlan et al., 1999) and in vitro (Chavis and Westbrook, 2001) studies, and reduces synaptic NMDA currents to single stimuli (this study) as well as bursts (Philpot et al., 2001a) of afferent activity. The reduction to single stimuli suggests that with activity, more NR2B-containing receptors are removed than NR2A-containing receptors are inserted, although differences in single-channel properties between NR2A and NR2B may be responsible.

Our results indicate that ligand binding to synaptic NR2B-containing receptors is sufficient to bring about the NR2B to NR2A replacement. This suggests that ligand binding by synaptic NR2B-containing receptors recruits an endocytosis apparatus that is linked to synaptic delivery of NR2A-containing receptors. Ligand-independent replacement of synaptic NR2B-containing receptors with recently synthesized NR2B-containing receptors must be a distinct process. Notably, ligand-

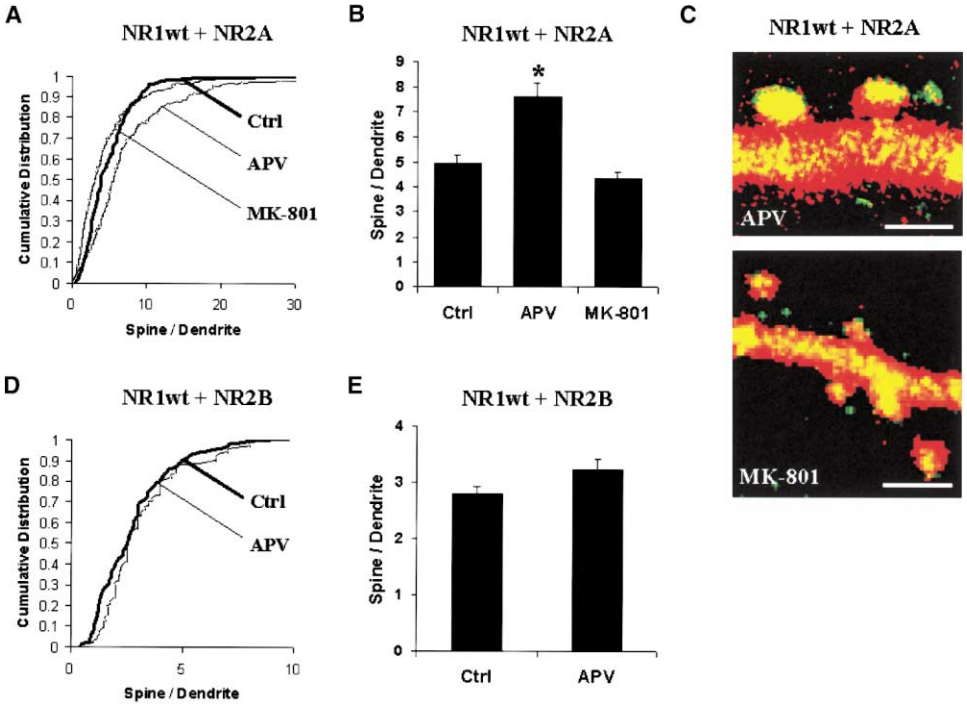

Figure 5. Receptor Delivery Blockade Detected Optically

(A–C) Block of functional insertion of NR2A-containing receptors leads to their accumulation in spines. Cumulative distribution for the spine/dendrite ratio from neurons expressing NR1-GFP, NR2A-GFP, and T1-Red, in control culture medium (thick line, 2 cells, 159 spines), culture medium with 100 μM APV (thin line, 6 cells, 334 spines), and culture medium with 10 μM MK-801 (thin line, 5 cells, 343 spines) (A), respectively. Average of spine/dendrite ratio for cells expressing NR1-GFP, NR2A-GFP, and T1-Red maintained in conditions indicated below ($p < 0.01$ for APV) (B). Overlap images from cells expressing NR1-GFP, NR2A-GFP, and T1-Red cultured with APV or MK-801 (C).

(D and E) Targeting of NR2B-containing receptors is not affected by NMDA-R activity. Cumulative distribution for the spine/dendrite ratio from neurons expressing NR1-GFP, NR2B-GFP, and T1-Red, in control culture medium (thick line, 2 cells, 146 spines), and culture medium with 100 μM APV (thin line, 2 cells, 98 spines) (D). Average of spine/dendrite ratio for cells expressing NR1-GFP, NR2B-GFP, and T1-Red for conditions indicated ($p > 0.05$) (E).

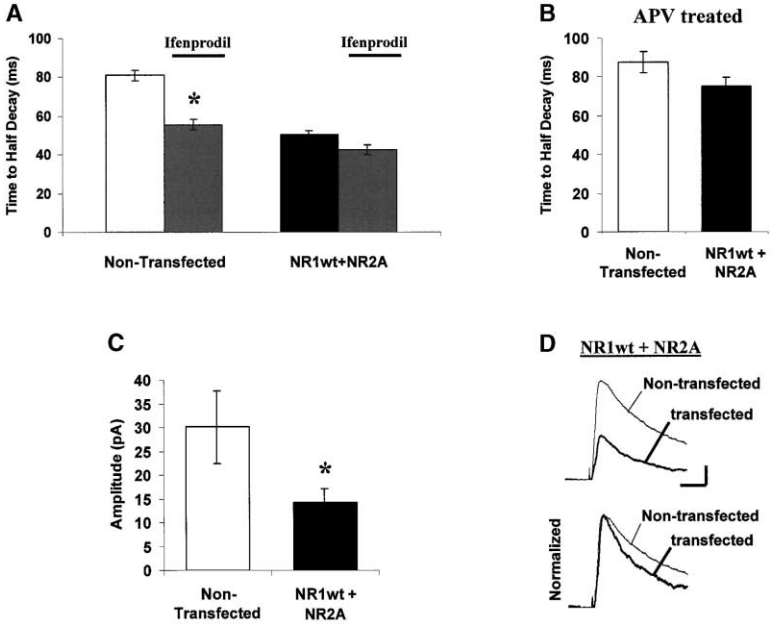

Figure 6. NR2A-Containing Receptors Replace Synaptic NR2B-Containing Receptors

(A) Decay of evoked EPSCs at +40 mV is faster in cells transfected with $NR1_{wt}$-GFP/NR2A-GFP (closed bar; n = 18) than nontransfected cells (open bar; n = 30); $p < 0.01$. After 30 min of ifenprodil (3 μM), time to half decay decreases in cells nontransfected (hatched bar; n = 14). $NR1_{wt}$-GFP/NR2A-GFP transfected cells become largely insensitive to ifenprodil (hatched bar; n = 6).

(B) APV blocks delivery of receptors and change in kinetics of EPSCs. Time to half decay from slices incubated in APV during expression of $NR1_{wt}$-GFP/NR2A-GFP (closed bar; n = 11) or nontransfected cells (open bar; n = 12; $p > 0.05$).

(C) Expression of $NR1_{wt}$-GFP/NR2A-GFP decreases NMDA-R currents. Amplitude of NMDA-R EPSC responses (+40 mV; measured between 110–160 ms after stimulation artifact) is reduced in cells expressing $NR1_{wt}$-GFP/NR2A-GFP (closed bar, n = 14) compared to response in a nearby nontransfected cell (open bar) recorded simultaneously ($p < 0.01$).

(D) Evoked NMDA-R-mediated synaptic responses recorded simultaneously in a cell expressing $NR1_{wt}$-GFP/NR2A-GFP and a nontransfected cell (scale bar = 50 ms, 10 pA).

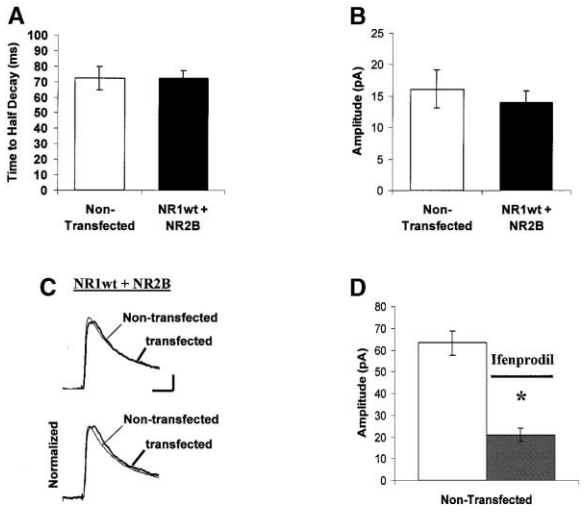

Figure 7. NR2B-Containing Receptors Do Not Replace Synaptic NR2A-Containing Receptors

(A) Time to half decay is not different in cells transfected with NR2B-containing receptors (closed bar; n = 17) relative to nontransfected cells (open bar; n = 17).

(B) Amplitude of NMDA-R EPSC responses is not significantly affected by expression of $NR1_{wt}$-GFP/NR2B-GFP (n = 20).

(C) Evoked NMDA-R-mediated synaptic responses recorded simultaneously in a cell expressing $NR1_{wt}$-GFP/NR2B-GFP and a nontransfected cell (scale bar = 50 ms, 10 pA).

(D) We confirmed that our preparation has synaptic NR2A-containing receptors by noting that a saturating NR2B-selective dose of ifenprodil (see Experimental Procedures) left a robust NMDA-R-mediated response (0.29 ± 0.03 of control; n = 14). Amplitude of NMDA-R EPSC from nontransfected cells before drug (open bar) or after 30 min of 3 μM ifenprodil (hatched bar; n = 16; $p < 0.01$).

dependent and ligand-independent forms of AMPA-R endocytosis have been described (Beattie et al., 2000; Lin et al., 2000). It will be of interest to examine, perhaps using exogenous puffing of NMDA, the rules governing NMDA-R delivery to dendritic (nonsynaptic) surfaces.

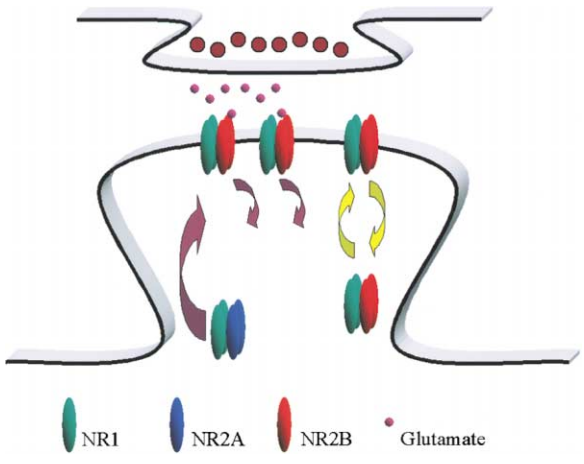

Figure 8. Model Describing Synaptic Trafficking of NMDA-Rs

Nonsynaptic NR2B-containing receptors replace synaptic NR2B-containing receptors. As NR2A expression increases (in a manner that requires ligand binding to synaptic receptors), NR2A-containing receptors replace synaptic NR2B-containing receptors. This reduces synaptic NMDA-R responses.

Our results show that spontaneous and, therefore, incoherent, synaptic activity can effect this switch from NR2B- to NR2A-containing receptors at synapses. Thus, while patterned coincident synaptic activity can promote calcium entry and synaptic plasticity (through LTP- or LTD-like processes), coincident or incoherent activity will suffice to drive an NR2B to NR2A switch. This switch occurs most effectively when NR2A levels are higher (at older ages) and serves to reduce NMDA-R responses. These effects may play a role in diminishing plasticity of AMPA-Rs (Carmignoto and Vicini, 1992; Crair and Malenka, 1995; Feldman et al., 1998; but, see Lu et al., 2001) observed in some brain regions as animals age. Since not all NMDA-Rs are bound by released transmitter (Mainen et al., 1999b), a ligand-driven switch in synaptic NMDA-R composition may enable a mechanism that "counts" trials and progressively limits plasticity of AMPA-R number.

Experimental Procedures

Construction and Neuronal Expression of Recombinant Receptors

The GFP coding sequence (enhanced GFP, Clontech, Palo Alto, California) was inserted after the predicted signal peptide cleavage site of the NMDA-R subunits. A restriction site that allowed the cloning of GFP was inserted after amino acid 21 in NR1, amino acid 26 in NR2A, and amino acid 31 in NR2B. Removal of the last six amino acids of NR2 subunits ($NR2_{\Delta PDZ}$ subunits) was made by PCR insertion of an early stop codon. All the subunits were cloned into pCI vector (Promega, Madison, Wisconsin). T1-Red was provided by Dr. Benjamin Glick, University of Chicago. Transfection of hippocampal slices was done using Helios Gene Gun (Bio-Rad, California), according to the manufacturer's protocol. Slices were prepared from postnatal day 6–7 animals, incubated in culture medium and 5% CO_2 for 4–5 days, and then transfected. After transfection, slices were cultured for ~60 hr to allow expression of recombinant proteins. For pharmacological experiments, drugs were added immediately after transfection and replenished every 24 hr.

Electrophysiology from Hippocampal Slice Neurons

Whole-cell recordings were obtained from transfected or nontransfected neurons under visual guidance using epi-fluorescence and transmitted light illumination. The recording chamber was perfused with artificial cerebrospinal fluid (ACSF) containing 119 mM NaCl, 2.5 mM KCl, 4 mM $CaCl_2$, 4 mM $MgCl_2$, 26 mM $NaHCO_3$, 1 mM NaH_2PO_4, 11 mM glucose, 0.1 mM picrotoxin, 2 μM 2-chloroadenosine (pH 7.4), and gassed with 5% CO_2/ 95% O_2. Recordings were made at room temperature (22–24°C). Patch recording pipettes (~4 MΩ) were filled with intracellular solution containing 115 mM cesium methanesulfonate, 20 mM CsCl, 10 mM HEPES, 2.5 mM $MgCl_2$, 4 mM Na_2ATP, 0.4 mM Na_3GTP, 10 mM sodium phosphocreatine, and 0.6 mM EGTA (pH 7.25) for current recordings or 115 mM potassium gluconate, 10 mM HEPES, 2 mM $MgCl_2$, 2 mM MgATP, 2 mM Na_2ATP, 0.3 mM Na_3GTP, and 20 mM KCl (pH 7.25) for voltage recordings. For miniature responses, ACSF with 0.5 M sucrose was puffed into the tissue. Whole-cell recordings were made with an Axopatch-1D amplifier (Axon Instruments, Foster City, California). Junction potentials were not corrected. For power spectrum analysis, 50–100 2 s responses were sampled in different concentrations of Mg^{2+}, and then APV was added to the bath. Traces were transformed with a fast fourier transform algorithm (IGOR Pro 3.15, Wavemetrics, Lake Oswego, Oregon), and power spectrum was calculated from those values. Only the frequencies relevant to NMDA-R transmission (0–20 Hz) are shown. The relevant range of frequencies was confirmed by power spectrum analysis of evoked NMDA-R-mediated responses and application of APV (100 μM) (data not shown). Synaptic responses were evoked by two bipolar electrodes with monophasic voltage pulses (1–10 V, 200 μs). The stimulating electrodes were placed over Schaffer collateral fibers approximately

300–500 μM from the CA1 cells. NMDA-R amplitude was measured 110–160 ms after stimulus artifact. Time to half decay for responses was measured from records obtained at +40 mV in the presence (Figure 6) or absence (Figure 7) of 2 μM NBQX. We established that 3 μM ifenprodil is a saturating NR2B-specific dose since (1) this dose reduced amplitude and timecourse of NMDA-R-mediated responses (see text) and (2) increasing concentrations (30 μM) failed to reduce the time to half decay of NMDA-R responses ($n = 6$). All results are reported as mean ± standard error of the mean (SEM), and statistical differences of these means were determined using either the Wilcoxon nonparametric test or Student's t test. Significance was set at $p \leq 0.05$.

Two-Photon Laser Scanning Microscopy

Transfected slices were placed in a chamber perfused with ACSF and imaged with a custom-made two-photon laser scanning microscope (Mainen et al., 1999a). Laser was tuned to a wavelength of 910 nm. Pyramidal neurons were chosen for inclusion in analysis based on dendritic characteristics. Image stacks (one image every 0.5 μM) were acquired and analyzed with Fluoview software 2.1 (Olympus). Using only the red channel (cytoplasmic T1-red expression), a region of interest (ROI) was drawn on a dendritic spine or on the adjacent dendritic shaft. Averaged maximum fluorescence intensity (F) was calculated for the ROI in each image in a stack for green and red channels; background (estimated from low ROI values in a stack) was subtracted.. The green signal was corrected for red leakage (10%) and normalized by the red signal to generate the volume-corrected GFP fluorescence, $F_{norm} = (F_{green} - [F_{red} \times 0.1])/F_{red}$. We computed F_{norm} for spine and adjacent dendrite to generate the volume-corrected spine to dendrite GFP ratio, $spineF_{norm}/dendF_{norm}$. Cumulative distribution curves for these values were generated for different conditions and were compared using the Kolmogorov-Smirnov test. Averages of $spineF_{norm}/dendF_{norm}$ were compared using Student's t test.

Transfection and Electrophysiology of HEK-293 Cells

HEK-293 cells were transfected with $NR1_{wt}$-GFP or $NR1_{N598R}$-GFP plus NR2A-GFP or NR2B-GFP using Lipofectin reagent (Gibco BRL, Life Technologies, Rockville, Maryland). After 36 hr, transfected cells were identified by fluorescence microscopy, and recordings were obtained with patch pipettes containing Cs-based intracellular solution. Responses at different holding potentials were evoked with brief pulses of glutamate (100 μM) and glycine (50 μM).

Coimmunoprecipitation Analysis

Organotypic hippocampal slices were infected with Sindbis virus carrying NR1-GFP. After 48 hr, slices were homogenized in 50 mM Tris (pH 8.8), 150 mM NaCl, 1X protease inhibitor cocktail containing EDTA (Complete tablets, Roche), and 1% deoxycholate. Homogenate was sonicated and incubated at 37°C for 40 min (Blahos and Wenthold, 1996). Insoluble material was removed by centrifugation. The supernatant was divided in two, diluted with 50 mM Tris (pH 7.5), protease inhibitor cocktail, and 0.1% Triton X-100, and then immunoprecipitated with monoclonal anti-GFP antibody (Roche) or anti-NR2A/B antibody (Chemicon). Anti-GFP antibody showed a very poor immunoprecipitation; therefore, anti-NR2 antibody was subsequently used. Immunoprecipitates were separated by SDS-PAGE and blotted with anti-NR1 antibody (Chemicon). A fraction of the supernatant, before and after the immunoprecipitation, was blotted with anti-NR2 antibody.

Acknowledgments

We thank N. Dawkins-Pisani for expert technical assistance, H. Cline for helpful comments on an earlier version of this manuscript, K. Svoboda for consultation on two-photon imaging, and S. Nakanishi and B. Glick for generously providing NMDA-R and enhanced dsRed clones, respectively. This study was funded by Alzheimer's foundation (A.B.), NIH (R.M.), and Alle Davis and Maxine Harrison Endowment (R.M.).

Received: January 11, 2002
Revised: May 31, 2002

References

Beattie, E.C., Carroll, R.C., Yu, X., Morishita, W., Yasuda, H., von Zastrow, M., and Malenka, R.C. (2000). Regulation of AMPA receptor endocytosis by a signaling mechanism shared with LTD. Nat. Neurosci. *3*, 1291–1300.

Blahos, J., 2nd, and Wenthold, R.J. (1996). Relationship between N-methyl-D-aspartate receptor NR1 splice variants and NR2 subunits. J. Biol. Chem. *271*, 15669–15674.

Burnashev, N., Schoepfer, R., Monyer, H., Ruppersberg, J.P., Gunther, W., Seeburg, P.H., and Sakmann, B. (1992). Control by asparagine residues of calcium permeability and magnesium blockade in the NMDA receptor. Science *257*, 1415–1419.

Calver, A.R., Robbins, M.J., Cosio, C., Rice, S.Q., Babbs, A.J., Hirst, W.D., Boyfield, I., Wood, M.D., Russell, R.B., Price, G.W., et al. (2001). The C-terminal domains of the GABA(b) receptor subunits mediate intracellular trafficking but are not required for receptor signaling. J. Neurosci. *21*, 1203–1210.

Carmignoto, G., and Vicini, S. (1992). Activity-dependent decrease in NMDA receptor responses during development of the visual cortex. Science *258*, 1007–1011.

Chavis, P., and Westbrook, G. (2001). Integrins mediate functional pre- and postsynaptic maturation at a hippocampal synapse. Nature *411*, 317–321.

Choi, D.W. (1995). Calcium: still center-stage in hypoxic-ischemic neuronal death. Trends Neurosci. *18*, 58–60.

Constantine-Paton, M., and Cline, H.T. (1998). LTP and activity-dependent synaptogenesis: the more alike they are, the more different they become. Curr. Opin. Neurobiol. *8*, 139–148.

Crair, M.C., and Malenka, R.C. (1995). A critical period for long-term potentiation at thalamocortical synapses. Nature *375*, 325–328.

Cummings, J.A., Mulkey, R.M., Nicoll, R.A., and Malenka, R.C. (1996). Ca^{2+} signaling requirements for long-term depression in the hippocampus. Neuron *16*, 825–833.

Dalva, M.B., Takasu, M.A., Lin, M.Z., Shamah, S.M., Hu, L., Gale, N.W., and Greenberg, M.E. (2000). EphB receptors interact with NMDA receptors and regulate excitatory synapse formation. Cell *103*, 945–956.

Dingledine, R., Borges, K., Bowie, D., and Traynelis, S.F. (1999). The glutamate receptor ion channels. Pharmacol. Rev. *51*, 7–61.

Feldman, D.E., Nicoll, R.A., Malenka, R.C., and Isaac, J.T. (1998). Long-term depression at thalamocortical synapses in developing rat somatosensory cortex. Neuron *21*, 347–357.

Flint, A.C., Maisch, U.S., Weishaupt, J.H., Kriegstein, A.R., and Monyer, H. (1997). NR2A subunit expression shortens NMDA receptor synaptic currents in developing neocortex. J. Neurosci. *17*, 2469–2476.

Garner, C.C., Nash, J., and Huganir, R.L. (2000). PDZ domains in synapse assembly and signalling. Trends Cell Biol. *10*, 274–280.

Huh, K.H., and Wenthold, R.J. (1999). Turnover analysis of glutamate receptors identifies a rapidly degraded pool of the N-methyl-D-aspartate receptor subunit, NR1, in cultured cerebellar granule cells. J. Biol. Chem. *274*, 151–157.

Kornau, H.C., Schenker, L.T., Kennedy, M.B., and Seeburg, P.H. (1995). Domain interaction between NMDA receptor subunits and the postsynaptic density protein PSD-95. Science *269*, 1737–1740.

Kutsuwada, T., Sakimura, K., Manabe, T., Takayama, C., Katakura, N., Kushiya, E., Natsume, R., Watanabe, M., Inoue, Y., Yagi, T., et al. (1996). Impairment of suckling response, trigeminal neuronal pattern formation, and hippocampal LTD in NMDA receptor epsilon 2 subunit mutant mice. Neuron *16*, 333–344.

Laurie, D.J., and Seeburg, P.H. (1994). Regional and developmental heterogeneity in splicing of the rat brain NMDAR1 mRNA. J. Neurosci. *14*, 3180–3194.

Lin, J.W., Ju, W., Foster, K., Lee, S.H., Ahmadian, G., Wyszynski, M., Wang, Y.T., and Sheng, M. (2000). Distinct molecular mechanisms and divergent endocytotic pathways of AMPA receptor internalization. Nat. Neurosci. *3*, 1282–1290.

Lu, H.C., Gonzalez, E., and Crair, M.C. (2001). Barrel cortex critical

period plasticity is independent of changes in NMDA receptor subunit composition. Neuron *32*, 619–634.

MacDonald, J.F., Bartlett, M.C., Mody, I., Pahapill, P., Reynolds, J.N., Salter, M.W., Schneiderman, J.H., and Pennefather, P.S. (1991). Actions of ketamine, phencyclidine and MK-801 on NMDA receptor currents in cultured mouse hippocampal neurones. J. Physiol. (Lond.) *432*, 483–508.

Mainen, Z.F., Maletic-Savatic, M., Shi, S.H., Hayashi, Y., Malinow, R., and Svoboda, K. (1999a). Two-photon imaging in living brain slices. Methods *18*, 231–239, 181.

Mainen, Z.F., Malinow, R., and Svoboda, K. (1999b). Synaptic calcium transients in single spines indicate that NMDA receptors are not saturated. Nature *399*, 151–155.

Meguro, H., Mori, H., Araki, K., Kushiya, E., Kutsuwada, T., Yamazaki, M., Kumanishi, T., Arakawa, M., Sakimura, K., and Mishina, M. (1992). Functional characterization of a heteromeric NMDA receptor channel expressed from cloned cDNAs. Nature *357*, 70–74.

Monyer, H., Sprengel, R., Schoepfer, R., Herb, A., Higuchi, M., Lomeli, H., Burnashev, N., Sakmann, B., and Seeburg, P.H. (1992). Heteromeric NMDA receptors: molecular and functional distinction of subtypes. Science *256*, 1217–1221.

Monyer, H., Burnashev, N., Laurie, D.J., Sakmann, B., and Seeburg, P.H. (1994). Developmental and regional expression in the rat brain and functional properties of four NMDA receptors. Neuron *12*, 529–540.

Mori, H., Masaki, H., Yamakura, T., and Mishina, M. (1992). Identification by mutagenesis of a Mg(2+)-block site of the NMDA receptor channel. Nature *358*, 673–675.

Mori, H., Manabe, T., Watanabe, M., Satoh, Y., Suzuki, N., Toki, S., Nakamura, K., Yagi, T., Kushiya, E., Takahashi, T., et al. (1998). Role of the carboxy-terminal region of the GluR epsilon2 subunit in synaptic localization of the NMDA receptor channel. Neuron *21*, 571–580.

Nakanishi, N., Axel, R., and Shneider, N.A. (1992). Alternative splicing generates functionally distinct N-methyl-D-aspartate receptors. Proc. Natl. Acad. Sci. USA *89*, 8552–8556.

Osten, P., Khatri, L., Perez, J.L., Köhr, G., Giese, G., Daly, C., Schulz, T.W., Wensky, A., Lee, L.M., and Ziff, E.B. (2000). Mutagenesis reveals a role for ABP/GRIP binding to GluR2 in synaptic surface accumulation of the AMPA receptor. Neuron *27*, 313–325.

Pagano, A., Rovelli, G., Mosbacher, J., Lohmann, T., Duthey, B., Stauffer, D., Ristig, D., Schuler, V., Meigel, I., Lampert, C., et al. (2001). C-terminal interaction is essential for surface trafficking but not for heteromeric assembly of GABA(b) receptors. J. Neurosci. *21*, 1189–1202.

Passafaro, M., Piech, V., and Sheng, M. (2001). Subunit-specific temporal and spatial patterns of AMPA receptor exocytosis in hippocampal neurons. Nat. Neurosci. *4*, 917–926.

Philpot, B.D., Sekhar, A.K., Shouval, H.Z., and Bear, M.F. (2001a). Visual experience and deprivation bidirectionally modify the composition and function of NMDA receptors in visual cortex. Neuron *29*, 157–169.

Philpot, B.D., Weisberg, M.P., Ramos, M.S., Sawtell, N.B., Tang, Y.P., Tsien, J.Z., and Bear, M.F. (2001b). Effect of transgenic overexpression of NR2B on NMDA receptor function and synaptic plasticity in visual cortex. Neuropharmacology *41*, 762–770.

Piccini, A., and Malinow, R. (2002). Critical PDZ interactions by GluR1 and GluR2 required at different subcellular sites. J. Neurosci., in press.

Quinlan, E.M., Philpot, B.D., Huganir, R.L., and Bear, M.F. (1999). Rapid, experience-dependent expression of synaptic NMDA receptors in visual cortex in vivo. Nat. Neurosci. *2*, 352–357.

Scott, D.B., Blanpied, T.A., Swanson, G.T., Zhang, C., and Ehlers, M.D. (2001). An NMDA receptor ER retention signal regulated by phosphorylation and alternative splicing. J. Neurosci. *21*, 3063–3072.

Sheng, M., and Pak, D.T. (2000). Ligand-gated ion channel interactions with cytoskeletal and signaling proteins. Annu. Rev. Physiol. *62*, 755–778.

Sheng, M., and Sala, C. (2001). Pdz domains and the organization of supramolecular complexes. Annu. Rev. Neurosci. *24*, 1–29.

Sheng, M., Cummings, J., Roldan, L.A., Jan, Y.N., and Jan, L.Y. (1994). Changing subunit composition of heteromeric NMDA receptors during development of rat cortex. Nature *368*, 144–147.

Shi, S., Hayashi, Y., Esteban, J.A., and Malinow, R. (2001). Subunit-specific rules governing ampa receptor trafficking to synapses in hippocampal pyramidal neurons. Cell *105*, 331–343.

Single, F.N., Rozov, A., Burnashev, N., Zimmermann, F., Hanley, D.F., Forrest, D., Curran, T., Jensen, V., Hvalby, O., Sprengel, R., and Seeburg, P.H. (2000). Dysfunctions in mice by NMDA receptor point mutations NR1(N598Q) and NR1(N598R). J. Neurosci. *20*, 2558–2566.

Sprengel, R., Suchanek, B., Amico, C., Brusa, R., Burnashev, N., Rozov, A., Hvalby, O., Jensen, V., Paulsen, O., Andersen, P., et al. (1998). Importance of the intracellular domain of NR2 subunits for NMDA receptor function in vivo. Cell *92*, 279–289.

Standley, S., Roche, K.W., McCallum, J., Sans, N., and Wenthold, R.J. (2000). PDZ domain suppression of an ER retention signal in NMDA receptor NR1 splice variants. Neuron *28*, 887–898.

Steigerwald, F., Schulz, T.W., Schenker, L.T., Kennedy, M.B., Seeburg, P.H., and Kohr, G. (2000). C-terminal truncation of NR2A subunits impairs synaptic but not extrasynaptic localization of NMDA receptors. J. Neurosci. *20*, 4573–4581.

Stocca, G., and Vicini, S. (1998). Increased contribution of NR2A subunit to synaptic NMDA receptors in developing rat cortical neurons. J. Physiol. (Lond.) *507*, 13–24.

Tovar, K.R., and Westbrook, G.L. (1999). The incorporation of NMDA receptors with a distinct subunit composition at nascent hippocampal synapses in vitro. J. Neurosci. *19*, 4180–4188.

Vissel, B., Krupp, J.J., Heinemann, S.F., and Westbrook, G.L. (2001). A use-dependent tyrosine dephosphorylation of NMDA receptors is independent of ion flux. Nat. Neurosci. *4*, 587–596.

Williams, K. (1993). Ifenprodil discriminates subtypes of the N-methyl-D-aspartate receptor: selectivity and mechanisms at recombinant heteromeric receptors. Mol. Pharmacol. *44*, 851–859.

Xia, H., Hornby, Z.D., and Malenka, R.C. (2001). An ER retention signal explains differences in surface expression of NMDA and AMPA receptor subunits. Neuropharmacology *41*, 714–723.

Zhu, J.J., Esteban, J.A., Hayashi, Y., and Malinow, R. (2000). Postnatal synaptic potentiation: delivery of GluR4-containing AMPA receptors by spontaneous activity. Nat. Neurosci. *3*, 1098–1106.

Zoghbi, H.Y., Gage, F.H., and Choi, D.W. (2000). Neurobiology of disease. Curr. Opin. Neurobiol. *10*, 655–660.

Zucker, R.S. (1999). Calcium- and activity-dependent synaptic plasticity. Curr. Opin. Neurobiol. *9*, 305–313.